

# Bifurcations in long Josephson junctions with second harmonic in the current-phase relation: Numerical study

Pavlina Atanasova<sup>1</sup> and Elena Zemlyanaya<sup>2</sup>

<sup>1</sup> University of Plovdiv, FMI, Plovdiv 4003, Bulgaria; [atanasova@uni-plovdiv.bg](mailto:atanasova@uni-plovdiv.bg)

<sup>2</sup> Laboratory of Information Technologies, Joint Institute for Nuclear Research  
141980 Dubna, Moscow Region, Russia; [elena@jinr.ru](mailto:elena@jinr.ru)

**Abstract.** Critical regimes in the long Josephson junction (LJJ) are studied within the frame of a model accounting the second harmonic in the current-phase relation (CPR). Numerical approach is shown to provide a good agreement with analytic results. Numerical results are presented to demonstrate the availabilities and advantages of the numerical scheme for investigation of bifurcations and properties of the magnetic flux distributions in dependence on the sign and value of the second harmonic in CPR.

**Keywords:** Long Josephson junction, double sine-Gordon equation, continuous analogue of Newton's method, numerical continuation, stability, bifurcations

## 1 Introduction

Physical properties of magnetic flux in Josephson junctions (JJs) play important role in the modern nanoelectronics. Generally, the current-phase relation (CPR) in the JJ is taken as the Fourier decomposition of sinuses [12]. For JJs of the “superconductor–insulator–superconductor” type, the CPR is close to a sinusoidal function of phase while another terms in the CPR Fourier decomposition are negligible. In those cases, the magnetic flux distributions are described by the sine-Gordon (SG) equation.

However, in a number of JJs models, the second harmonic contribution of the CPR Fourier expansion should be accounted, see for example, [14, 9, 10]. In the frame of corresponding models the magnetic flux distributions satisfy the following double sine-Gordon equation:

$$\varphi'' - \ddot{\varphi} - \alpha\dot{\varphi} = a_1 \sin \varphi + a_2 \sin 2\varphi - \gamma, \quad t > 0, \quad x \in (-l, l). \quad (1)$$

Here and below the prime means a derivative with respect to the coordinate  $x$  and the dot – with respect to the time  $t$ . The case of the overlap-contact of a finite length yields the following form of boundary conditions

$$\varphi'(\pm l, t) = h_e. \quad (2)$$

In (1),(2),  $\varphi$  is a magnetic flux distribution,  $h_e$  – an external magnetic field,  $\gamma$  – the external current,  $\alpha \geq 0$  – the dissipation coefficient,  $l$  is the semilength of the junction,  $a_1$  and  $a_2$  are parameters corresponding the contribution of 1st and 2nd harmonic in CPR, respectively. The sign of  $a_2$  can be positive or negative in the frame of different physical applications.

Static regimes of the magnetic flux distributions are described by the non-linear boundary problem [12, 11, 7]:

$$-\varphi'' + a_1 \sin \varphi + a_2 \sin 2\varphi - \gamma = 0, \quad x \in (-l, l), \quad \varphi'(\pm l) = h_e \quad (3)$$

that follows from a necessary condition for the full energy functional extremum. Bifurcations of  $\varphi$  correspond the transitions of junction from superconducting to resistive state where the voltage measurement changes from zero to nonzero value. Stable distributions correspond to superconductive state where the voltage is equal to zero.

The stability analysis of solution  $\varphi(x, p)$  where  $p = (l, a_1, a_2, h_e, \gamma)$  is a vector of parameters) can be reduced to the numerical solution of the corresponding Sturm-Liouville problem (SLP) [8, 13]:

$$-\psi'' + q(x)\psi = \lambda\psi, \quad \psi'(\pm l) = 0, \quad q(x) = a_1 \cos \varphi + 2a_2 \cos 2\varphi. \quad (4)$$

The case of positive minimal eigenvalue  $\lambda_0(p) > 0$  corresponds the minimum of the distribution energy and, hence, the stable solution  $\varphi$ . In case  $\lambda_0(p) < 0$  solution  $\varphi(x, p)$  is unstable. The case  $\lambda_0(p) = 0$  indicates the bifurcation (the transition of junction from superconducting to resistive state) with respect to one of parameters  $p$ .

Our numerical approach is based on the consideration of Eqs.(3),(4) as unique problem with respect to functions  $\varphi$ ,  $\psi$ , and one of the parameters  $p$ . In comparison with a standard direct numerical simulation of Eq.(1), this method simplifies an obtaining of the dependence of critical current  $\gamma_{cr}$  on external magnetic field  $h_e$  – an important physical observable measured in experiments. This idea was successfully applied to reproduce critical states in different models described by SG (i.e. with  $a_2 = 0$ ), see for example [13, 1] and references there. We extend this technique for the case of nonzero  $a_2$  and investigate the effect of the second harmonic accounting on the critical magnetic flux distributions.

Beside, our numerical scheme is furnished with a continuation algorithm [17, 5] providing analysis of interconnection between coexisting (stable and unstable) distributions. We study the critical curves and the stability areas of the corresponding solutions under the influence of the second harmonic in CPR. In Sect. 2 we describe details of our numerical approach. Results of numerical study are discussed in Sect. 3. Concluding remarks are given in Sect. 4.

## 2 Numerical approach

Supplying the system (3),(4) with a normalization condition for the eigenfunction  $\psi(x)$  of SLP (4)

$$\int_{-l}^{+l} \psi^2(x) dx = 1. \quad (5)$$

we proceed the nonlinear problem at  $x \in (-l; l)$ . The system (3-5) is considered as the unified nonlinear functional equation for the functions  $\varphi(x)$ ,  $\psi(x)$ , and one of the five parameters  $p$  (which we denote by  $\xi$ ). The other four parameters  $\bar{p} \in p$  are assumed to be known. Thus, the system (3-5) can be rewritten in a vector form as follows:

$$\mathcal{F}(y, \bar{p}) = 0, \quad (6)$$

where  $y = (\varphi, \psi, \xi)$  is unknown element in Banach space and  $\bar{p}$  is the set of parameters.

In the simplest case, when all the elements of the vector  $p$  are defined, the problem is split into independent subsystems (3) and (4-5). The eigenvalue  $\lambda$  is to be found, which corresponds to the solution  $\varphi(x)$  of (3). This approach was applied in our papers [2, 6, 3].

In case the eigenvalue of SLP is assumed to be fixed  $\lambda = 0$ , we obtain the closed system (3-5) with respect to the unknown Banach element  $y$ . Considering the case  $\xi = \gamma$  and solving the problem (6) with respect to  $y = (\varphi, \psi, \gamma)$  yields the value  $\gamma = \gamma_{cr}$  that corresponds the bifurcation magnetic flux distribution  $\varphi$ . The bifurcation solution  $y$  is path-followed in the continuation parameter  $h_e$  and the critical dependence  $\gamma_{cr}(h_e)$  is determined.

In the case  $\xi = \gamma$  or  $\xi = h_e$  the continuation of the bifurcation solution in the parameter  $a_2$  produces the dependence of stability region on external current  $\gamma$  or on external magnetic field  $h_e$ .

Below, we present the Newtonian iteration scheme for numerical solution of the problem (6) for the case of  $\xi = \gamma$ .

The continuous analog of Newton's method (CANM) [13] reduces the problem (6) to the auxiliary linear problem:

$$\frac{\partial \mathcal{F}}{\partial y} w + \mathcal{F}(y) = 0, \quad (7)$$

where  $w$  denotes the iteration increment of  $y$ :  $w = (u, v, \Gamma)$ , and  $\partial \mathcal{F} / \partial y$  is the Frechet derivative. For each element  $\mathcal{F}_i$  of the vector-function  $\mathcal{F}$  we have

$$\frac{\partial \mathcal{F}_1}{\partial y} w = -u'' + qu - \Gamma, \quad (8)$$

$$\frac{\partial \mathcal{F}_2}{\partial y} w = u'(-l), \quad \frac{\partial \mathcal{F}_3}{\partial y} w = u'(l), \quad (9)$$

$$\frac{\partial \mathcal{F}_4}{\partial y} w = -v'' + ru\psi + qv - \lambda v, \quad r = -a_1 \sin \varphi - 4a_2 \sin 2\varphi \quad (10)$$

$$\frac{\partial \mathcal{F}_5}{\partial y} w = v'(-l), \quad \frac{\partial \mathcal{F}_6}{\partial y} w = v'(l), \quad (11)$$

$$\frac{\partial \mathcal{F}_7}{\partial y} w = 2 \int_{-l}^l \psi v dx. \quad (12)$$

Finally, we obtain the linear system with respect to the unknowns  $w = (u, v, \Gamma)$ :

$$-u'' + qu - \Gamma - \varphi'' + f = 0, \quad (13)$$

$$u'(\pm l) + \varphi'(\pm l) - h_e = 0, \quad (14)$$

$$-v'' + ru\psi + qv - \lambda v - \psi'' + q\psi - \lambda\psi = 0, \quad (15)$$

$$v'(\pm l) + \psi'(\pm l) = 0, \quad (16)$$

$$2 \int_{-l}^l \psi v dx + \int_{-l}^l \psi^2 dx - 1 = 0. \quad (17)$$

Solutions  $u(x)$  and  $v(x)$  of the system (13-17) are decomposed in a form of linear combination

$$u(x) = u_1(x) + \Gamma u_2(x), \quad v(x) = v_1(x) + \Gamma v_2(x), \quad (18)$$

where  $x \in (-l; l)$  and  $u_1, u_2, v_1, v_2$  are solutions, respectively, of the following boundary-value problems:

$$-u_1'' + qu_1 - \varphi'' + f = 0, \quad u_1'(\pm l) + \varphi'(\pm l) - h_e = 0, \quad (19)$$

$$-u_2'' + qu_2 - 1 = 0, \quad u_2'(\pm l) = 0, \quad (20)$$

$$-v_1'' + r\psi u_1 + (q - \lambda)v_1 - \psi'' + (q - \lambda)\psi = 0, \quad v_1'(\pm l) + \psi'(\pm l) = 0, \quad (21)$$

$$-v_2'' + r\psi u_2 + (q - \lambda)v_2 = 0, \quad v_2'(\pm l) = 0, \quad (22)$$

Quantity  $\Gamma$  can be determined from the following expression:

$$2 \int_{-l}^l \psi v_1 dx + 2\Gamma \int_{-l}^l \psi v_2 dx + \int_{-l}^l \psi^2 dx - 1 = 0. \quad (23)$$

The above formulae (18-23) define the following sequence of calculations at each newtonian iteration for the fixed value of the continuation parameter  $h_e$ . Let us assume, at  $n$ -th iteration we have  $n$ -th approximation of solution  $\varphi^n(x)$ ,  $\psi^n(x)$  and  $\gamma^n$ . At  $(n+1)$ -th iteration:

1. We calculate the functions  $u_1^n(x)$  and  $u_2^n(x)$  from the linear boundary-value problems (19) and (20).
2. Then we solve linear boundary-value problems (21) and (22) with obtained functions  $u_1^n(x)$  and  $u_2^n(x)$  and determine solutions  $v_1^n(x)$  and  $v_2^n(x)$ .
3. Quantity  $\Gamma^n$  is calculated using Eq.(23).
4. The  $(n + 1)$ -th approximation of  $\varphi^{n+1}(x)$ ,  $\psi^{n+1}(x)$  and  $\gamma^{n+1}$  is defined by means of the formulas

$$\varphi^{n+1}(x) = \varphi^n(x) + \tau_n [u_1^n(x) + \Gamma^n u_2^n(x)], \quad (24)$$

$$\psi^{n+1}(x) = \psi^n(x) + \tau_n [v_1^n(x) + \Gamma^n v_2^n(x)], \quad (25)$$

$$\gamma^{n+1} = \gamma^n + \tau_n \Gamma^n, \quad (26)$$

where the iteration parameter  $\tau_n$  is calculated as follows [15]:

$$\tau_n = \max \left( \tau_{min}, \frac{\delta_n(0)}{\delta_n(0) + \delta_n(1)} \right). \quad (27)$$

Here  $\tau_{min}$  is a fixed minimal value of parameter  $\tau_n$  ( $0 < \tau_{min} \leq 1$ );

$$\delta_n(0) \equiv \|\mathcal{F}(\varphi^n, \psi^n, \gamma^n)\|, \quad \delta_n(1) \equiv \|\mathcal{F}(\bar{\varphi}^{n+1}, \bar{\psi}^{n+1}, \bar{\gamma}^{n+1})\|$$

where  $\|\cdot\|$  means the standard  $C$ -norm and  $\bar{\varphi}^{n+1}, \bar{\psi}^{n+1}, \bar{\gamma}^{n+1}$  are obtained by means Eqs.(24-26) with  $\tau_n = 1$ .

5. The iterations are finished when the inequality  $\|\mathcal{F}\| \leq \epsilon$  holds true, where  $\epsilon > 0$  is a small number chosen beforehand.

Convergence of the CANM-based iteration process is proved in [16].

For numerical solution of the linear boundary-value problems (19-22) at each Newtonian iteration, we apply Numerov's finite-difference approximation of the 4th order accuracy [4].

### 3 Numerical results

Together with the well-known distributions (standardly called  $M_\pi$  and  $M_0$ ) the nonzero  $a_2$  in Eq.(3) gives a rise another uniform state (called  $M_{\pm ac}$  in [6]). Stability and bifurcations of  $M_{\pm ac}$  have been investigated in [6, 2].

New fluxon solution inspired by the second harmonic contribution was observed in direct numerical simulation [9] and denoted "small fluxon" in contradiction to the standard "large fluxon" solution  $\Phi^1$ . Later, the "small fluxon" was reproduced in [2] in the frame of CANM-based numerical approach.

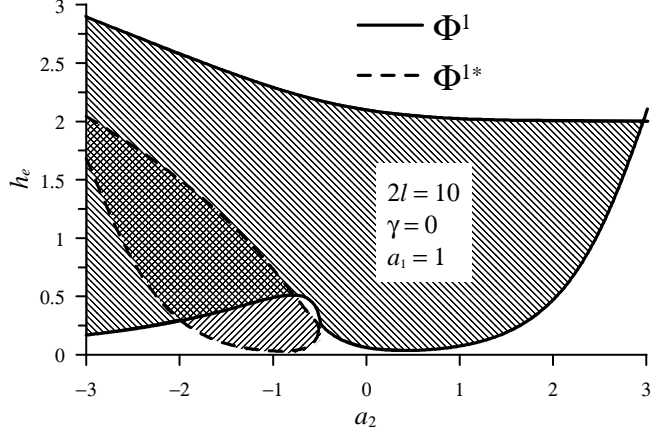
"Large fluxon"  $\Phi_1$  and "small fluxon" are characterized, respectively, with  $N = 1$  and  $N = 0$  where the quantity  $N$  (denoted "number of fluxons" in [6]) is determined as follows

$$N = \frac{1}{2l\pi} \int_{-l}^l \varphi(x) dx. \quad (28)$$

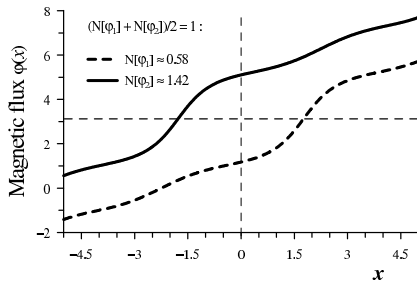
One more  $a_2$ -inspired one-fluxon solution  $\Phi^{1*}$  (existing at  $a_2 < -0.5$ ) was obtained in [4]. As the standard solution  $\Phi^1$ , the  $\Phi^{1*}$  fluxon characterized by the "number of fluxons"  $N = 1$

Figure 1 exhibits the full stability chart of two fluxons:  $\Phi^{1*}$  and  $\Phi^1$  on the  $(h_e, a_2)$ -plane for the case  $a_1 = 1$ . Stability domains of  $\Phi^1$  and  $\Phi^{1*}$  are bounded, respectively, by solid and dashed curves. In the region where two stability domains overlap, the different stable fluxon distributions coexist.

Our numerical study shows that, beside of bound states of two, three and more identical fluxons  $\Phi^1$ , Eq.(3) holds the stable the mixed bound states of different types of fluxons. Stable mixed solutions  $\varphi_1$  and  $\varphi_2$  are shown in figs 2,3 for  $h_e = 0.6$ ,  $a_1 = 1$ ,  $a_2 = -1$ . They are characterized by  $(N[\varphi_1] + N[\varphi_2])/2 = 1$  while quantities  $N[\varphi_1]$  and  $N[\varphi_2]$  are fractional. Note that stability of the mixed



**Fig. 1.** Bifurcation diagram of two fluxons  $\Phi^1$  and  $\Phi^{1*}$  at the plane of parameters  $a_2$  and  $h_e$ . Here  $a_1 = 1$ ,  $2l = 10$ ,  $\gamma = 0$ .



**Fig. 2.** The magnetic flux distribution  $\varphi(x)$  for the stable mixed bound state of two fluxons with  $h_e = 0.6$ ,  $a_1 = 1$ ,  $a_2 = -1$ ,  $2l = 10$ ,  $\gamma = 0$ .

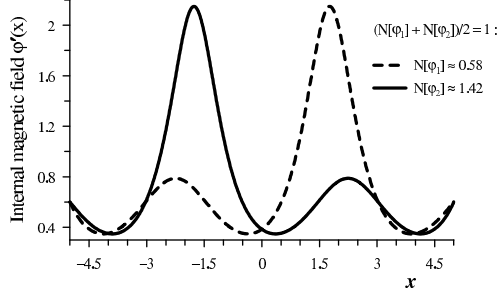


**Fig. 3.** The internal magnetic field distribution  $\varphi'(x)$  for the stable mixed bound state of two fluxons with  $h_e = 0.6$ ,  $a_1 = 1$ ,  $a_2 = -1$ ,  $2l = 10$ ,  $\gamma = 0$ .

bound states depends on  $a_2$  and  $h_e$ . For growing  $a_2$  this solution stabilizes for sufficiently small  $h_e$ .

Figures 4 and 5 demonstrate the critical current curves  $\gamma_{cr}(h_e)$  for  $a_2 = 0$ ,  $a_2 = 0.3$ , and  $a_2 = 1$ . Maximal value of the critical current corresponds the  $M_0$  distribution for  $h_e = 0$ . Another portions of critical current curve (for growing  $h_e$ ) correspond, sequentially, one-fluxon solution  $\Phi^1$ , two-fluxon solution  $\Phi^2$ , three-fluxon solution  $\Phi^3$ , etc. Here, we present the case of relatively short junctions  $2l = 1/\pi$  in order to show that our results are in a good agreement with results of direct numerical simulation of Eq. (1) [9]. Note, for longer  $l$  and for growing  $a_2$  a complexity of the  $\gamma_{cr}(h_e)$  dependence increases, see fig.5.

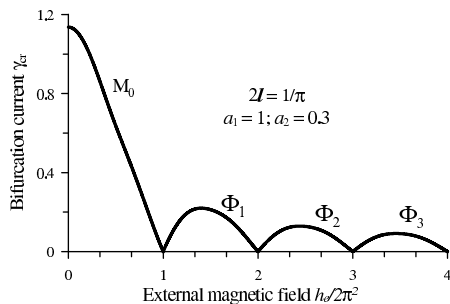


**Fig. 4.** Critical curves for short junction  $2l = 1/\pi$  with  $a_1 = 1$  and  $a_2 = 0.3$ .

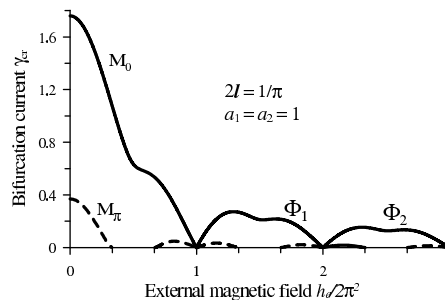


**Fig. 5.** Critical curves for the short junction  $2l = 1/\pi$  with  $a_1 = a_2 = 1$ .

## 4 Conclusions

The aim of this contribution is to present the numerical scheme for the bifurcation analysis of static magnetic flux distributions in long Josephson junctions described by double sine-Gordon equation (1). Instead of direct numerical simulation of partial differential equation (1) we numerically solve the boundary problem for the system of nonlinear ordinary differential equations.

It is shown that our numerical approach allows one to obtain new fluxon distributions of Eq. (1), to investigate their stability and bifurcations and to construct the critical current dependence, important physical characteristic of LJJs.

The work is partially supported in the frame of the Program for collaboration of JINR-Dubna and Bulgarian scientific centers “JINR – Bulgaria”. E.V.Z. was partially supported by RFFI under grant 12-01-00396a. P.Kh.A. is partially supported by the project NI11-FMI-004.

## References

1. Atanasova, P.Kh., Boyadzhiev, T.L., Dimova, S.N. Numerical Modeling of Critical Dependence for Symmetric Two-Layer Josephson Junctions, *Comput. Maths. and Math. Phys.* vol. 46, No. 4, pp. 666-679 (2006)
2. Atanasova, P.Kh., Boyadjiev, T.L., Shukrinov, Yu.M., Zemlyanaya E.V., Seidel, P.: Influence of Josephson current second harmonic on stability of magnetic flux in long junctions. arXiv:1007.4778v1, 2010; *J. Phys. Conf. Ser.* 248, 012044 (2010)
3. Atanasova, P.Kh., Boyadjiev, T.L., Shukrinov, Yu.M., Zemlyanaya E.V.: Numerical study of magnetic flux in the LJJ model with double sine-Gordon equation. arXiv:1007.4778v1 (2010); *Lecture Notes in Computer Sciences* 6046, 347-352 (2011)
4. Atanasova, P.Kh., Boyadjiev, T.L., Shukrinov, Yu.M., Zemlyanaya E.V.: Numerical investigation of the second harmonic effects in the LJJ. arXiv:1005.5691v1 (2010); in *Proc. the FDM'10 Conf. (Lozenetz, Bulgaria, July 2010)*, eds. M.Koleva and L.Vulkov, Rouse, pp. 1-8 (2011)

5. Atanasova, P.Kh., Zemlyanaya, E.V., Shukrinov Yu.M.: Numerical study of fluxon solutions of sine-Gordon equation under the influence of the boundary conditions. *Lecture Notes in Computer Sciences* 7125, 201-206 (2012)
6. Atanasova, P.Kh., Zemlyanaya, E.V., Boyadjiev, T.L., Shukrinov, Yu.M.: Numerical modeling of long Josephson junctions in the frame of double sine-Gordon equation. *Mathematical Models and Computer Simulations*. Vol. 3, No. 3, pp. 388-397 (2011)
7. Buzdin, A., Koshelev, A.E.: Periodic alternating 0-and  $\pi$ -junction structures as realization of  $\varphi$ -Josephson junctions. *Phys. Rev. B*. vol. 67, p. 220504(R) (2003)
8. Galpern, Yu.S., Filippov, A.T.: Joint solution states in inhomogeneous Josephson junctions. *Sov. Phys. JETP*. vol. 59, p. 894 (Russian) (1984)
9. Goldobin, E., Koelle, D., Kleiner, R., Buzdin, A.: Josephson junctions with second harmonic in the current-phase relation: Properties of junctions. *Phys. Rev. B*. vol. 76, 224523 (2007)
10. Goldobin, E., Koelle, D., Kleiner, R., Mints, R.G. Josephson junction with magnetic-field tunable ground state. *Phys. Rev. Lett.* vol. 107, 227001 (2011)
11. Hatakenaka, N., Takayanagi, H., Kasai, Yo., Tanda, S.: Double sine-Gordon fluxons in isolated long Josephson junction. *Physica B*. vol. 284-288, pp. 563-564 (2000)
12. Likharev, K.K.: Introduction in Josephson junction dynamics, M. Nauka, GRFML (Russian) (1985)
13. Puzynin, I. V., et al.: Methods of Computational Physics for Investigation of Models of Complex Physical Systems. *Physics of Particles and Nuclei*. vol. 38, No. 1, pp. 70-116 (2007)
14. Ryazanov, V.V., et al.: Coupling of two superconductors through a ferromagnet: evidence for a  $\pi$  junction. *Phys. Rev. Lett.* vol. 36, pp. 2427-2430 (2001)
15. Ermakov, V.V, Kalitkin, N.N.: The optimal step and regularisation for Newton's method, *Comput. Maths. and Math. Phys.* vol. 21, No. 2, pp. 235-242 (1981)
16. Zhanlav, T., Puzynin, I.V.: On iterations convergence on the base of continuous analog of Newton's method. *Comput. Maths. and Math. Phys.* vol. 32, No. 6, pp. 729-737 (1992)
17. Zemlyanaya, E.V., Barashenkov, I.V.: Numerical study of the multisoliton complexes in the damped-driven NLS. *Math. Modelling* (Russian) vol. 16, No. 3, pp. 3-14 (2004)